

NASA Technical Memorandum 106365
ICOMP-93-35

1N-34
191157
23 P

Parametric Resonant Triad Interactions in a Free Shear Layer

N94-15751

Unclass

G3/34 0191157

R. Mallier
McGill University
Montreal, Quebec, Canada

and

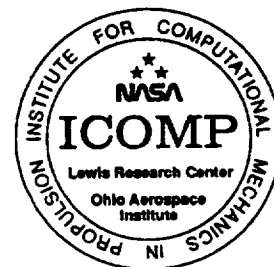
S.A. Maslowe
Institute for Computational Mechanics in Propulsion
Lewis Research Center
Cleveland, Ohio

and *McGill University*
Montreal, Quebec, Canada

(NASA-TM-106365) PARAMETRIC
RESONANT TRIAD INTERACTIONS IN A
FREE SHEAR LAYER (NASA) 23 P

October 1993

NASA



PARAMETRIC RESONANT TRIAD INTERACTIONS IN A FREE SHEAR LAYER

R. Mallier
McGill University
Department of Mathematics and Statistics
Montreal, Quebec, Canada H3A 2K6

and

S.A. Maslowe
Institute for Computational Mechanics in Propulsion
Lewis Research Center
Cleveland, Ohio 44135

and McGill University
Department of Mathematics and Statistics
Montreal, Quebec, Canada H3A 2K6

ABSTRACT

We investigate the weakly nonlinear evolution of a triad of nearly-neutral modes superimposed on a mixing layer with velocity profile $\bar{u} = u_m + \tanh y$. The perturbation consists of a plane wave and a pair of oblique waves each inclined at approximately 60° to the mean flow direction. Because the evolution occurs on a relatively fast time scale, the critical layer dynamics dominate the process and the amplitude evolution of the oblique waves is governed by an integro-differential equation. The long-time solution of this equation predicts very rapid (exponential of an exponential) amplification and we discuss the pertinence of this result to vortex pairing phenomena in mixing layers.

1. INTRODUCTION.

Transition to turbulence in unbounded, incompressible mixing layers occurs in several stages. The initial instability, according to most experiments, is primarily two-dimensional, an observation consistent with linear stability theory where the largest growth rates correspond to plane waves propagating in the mean flow direction. Nonlinearity results in eventual saturation of the linearly most amplified wave and as this mode tends toward equilibration, a subharmonic wave having one-half the frequency of the initial disturbance makes its appearance (as do higher harmonics). This intriguing phenomenon is observed in smoke visualization experiments and is also apparent from hot-wire signals. It is usually described as "vortex pairing", i.e., the initial disturbance manifests itself as a row of vortices and adjacent pairs of vortices begin to roll around each other, finally coalescing into a single vortex.

The first experimental observations of vortex pairing were reported around 1960 and concerned laminar flows undergoing transition. It was not until the mid 1970s, however, that interest in the subject greatly expanded because of the first reports that this process occurs in turbulent mixing layers, as well, and is a dominant factor contributing to the downstream growth of the mixing layer. A comprehensive review of these experiments, as well as the early theoretical developments, can be found in the survey article by Ho and Huerre (1984). The same article also discusses some early observations of three-dimensional structures which take the form of counter-rotating vortices whose axes are in the direction of the mean flow. Considerable experimental work has been reported more recently on the three-dimensional structures. Huang and Ho (1990), for example, discuss spanwise wavelength doubling due to merging of the counter-rotating streamwise vortices.

The present paper is, of course, concerned with the mathematical analysis of these phenomena. A principal contribution toward that end is contained in ideas put forward by Kelly (1967) who showed that certain features observed in the early stages of vortex pairing could be modelled (and in some cases predicted) by studying the resonant interaction of two disturbances whose wavenumbers are in the ratio 2:1. The shorter wave in Kelly's analysis was taken to be periodic in space and time (i.e. neutral) whereas the long wave had, initially, a much smaller amplitude. Its subharmonic instability corresponds to the onset of pairing. Subsequently, Patnaik *et al.* (1976) performed numerical simulations of instability in a stratified mixing layer and showed that the entire pairing process could be modelled by following the temporal evolution of two interacting Fourier modes with

wavenumbers related as in Kelly's analysis.

Patnaik *et al.* discovered by trial and error that the interaction of two such modes was greatly influenced by the phase relationship between them and in one limit it is very weak (they termed this a "shredding interaction"). This sensitivity to the relative phase is in fact a feature of several weakly nonlinear resonant interaction theories and had been noted earlier in the context of capillary-gravity waves, as pointed out by Collins and Maslowe (1989). There are some potentially important technological consequences of the foregoing remarks because they suggest that by forcing the interacting modes with the desired phase relationship the rate of growth of the mixing layer can be controlled. This has been verified experimentally by Hussain and Hussain (1989).

The role of the relative phase was emphasized in an extension of Kelly's analysis by Monkewitz (1988) in which the fundamental mode was taken to be nearly neutral, whereas the subharmonic was spatially amplified. Even though the analysis is described as weakly nonlinear, the wavenumber α of the subharmonic was taken to have an imaginary part as in linear spatial stability theory because the author argues that the amplification factor, $-\alpha_i$, is too large to be accounted for by introducing a slow scale in the flow direction. Despite this inconsistency, comparison of some experiments with an "ad hoc" version of the theory taking into account weakly nonparallel effects shows reasonable qualitative agreement.

We do not believe that this is entirely fortuitous and in the present paper seek to formulate a rational analysis of resonant triads in a $\tanh y$ mixing layer. There are two keys to overcoming the obstacles cited by Monkewitz. The first is to employ a pair of oblique waves as the subharmonic so that all modes are neutral or at least nearly-neutral in an asymptotic sense. The resulting analysis which is related to studies by Wu (1992) of the Stokes layer and Goldstein and Lee (1992) of the adverse pressure gradient boundary layer is greatly facilitated in the example of the $\tanh y$ mixing layer by the availability of a closed-form neutral solution. Consequently, we are able to determine explicitly the coefficients of all terms in our amplitude equations without the need for numerical computation or long-wave expansions.

The second key is to use an appropriate analysis of the critical layer (a thin layer centered on the point y_c where the phase speed of the interacting waves is equal to the mean flow velocity) because the critical layer dynamics seem to dominate the evolution of the flow for a significant distance beyond the region of exponential amplification of the linearly most unstable wave. This was demonstrated convincingly by Hultgren (1992) who

employed a quasi-equilibrium nonlinear critical layer analysis downstream of the initial region of linear instability. In addition, weakly nonparallel effects were taken into account outside of the critical layer. Excellent agreement was obtained with several experiments up to the onset of vortex pairing. Briefly, one reason why such favourable comparisons can be achieved despite the questionable small-amplification assumption in the theory is that due to the spreading of the mixing layer the wavenumber on a nondimensional basis increases as the shear layer thickens and it approaches the neutral value near saturation ($\alpha_n = 1$ for a $\tanh y$ mixing layer).

An extension of Hultgren's analysis to include resonant interactions would in all likelihood lead to the best agreement with the experimental data available to date. However, because simulating these experiments is not our primary objective, we will employ a procedure that is appropriate to the early stages of pairing and that will facilitate comparison with numerical simulations of the Navier-Stokes equations. Specifically, we will employ what some authors have termed a non-equilibrium critical layer in which the flow evolves on a relatively fast time scale, i.e., $\varepsilon^{1/4}t$, where ε is an amplitude parameter, rather than $\varepsilon^{1/2}t$ which would be the slow scale for a nonlinear critical layer (see, e.g., Maslowe (1986) for a review of critical layer theories). Although a spatial theory using a slow $\varepsilon^{1/4}x$ scale would be appropriate for comparison with experiments, most numerical simulations are based on the temporal theory for reasons of economy. In any case, as shown in Section 5, our amplitude equations can be converted easily to the spatial case.

Due to the above choice of slow time scale, our critical layer equations can be characterized as unsteady and weakly nonlinear. According to the amplitude equations that result, the nearly-neutral plane wave will amplify exponentially as in linear theory, but the oblique mode amplification is governed by an integro-differential equation of the sort first derived by Hickernell (1984) in the context of a mixing layer on the beta plane. The asymptotic solution of this equation for very large times is shown in Section 4 to exhibit exponential of an exponential amplification. Finally, in Section 5, we compare our results with some numerical simulations and also discuss their possible relevance to experiments.

2. FORMULATION AND OUTER EXPANSION.

We consider the stability of the dimensionless mixing layer profile

$$\bar{u}(y) = u_m + \tanh y \quad (2.1)$$

by adding a small perturbation of $O(\varepsilon)$, where $\varepsilon \ll 1$ is a dimensionless amplitude parameter. The equations of motion can be written

$$\frac{\partial \mathbf{q}}{\partial t} + (\mathbf{q} \cdot \nabla) \mathbf{q} = -\nabla p \quad (2.2)$$

and

$$\nabla \cdot \mathbf{q} = 0, \quad (2.3)$$

where we have supposed the fluid to be inviscid and incompressible. The temporal stability problem is independent of u_m , the mean velocity in (2.1), so we will set $u_m = 0$ until later in the paper when we discuss the spatial case.

The velocity components $\mathbf{q} = (\bar{u} + \varepsilon u, \varepsilon v, \varepsilon w)$ and the perturbation pressure εp are expanded as follows:

$$u = u^{(1)} + \varepsilon^{1/4} u^{(2)} + \varepsilon^{1/2} u^{(3)} + \dots \quad (2.4)$$

$$v = v^{(1)} + \varepsilon^{1/4} v^{(2)} + \varepsilon^{1/2} v^{(3)} + \dots \quad (2.5)$$

$$w = w^{(1)} + \varepsilon^{1/4} w^{(2)} + \varepsilon^{1/2} w^{(3)} + \dots \quad (2.6)$$

and

$$p = p^{(1)} + \varepsilon^{1/4} p^{(2)} + \varepsilon^{1/2} p^{(3)} + \dots \quad (2.7)$$

In the linearized problem, perturbations proportional to $\exp[i(\alpha x + \beta z - \alpha c t)]$ are considered and the y -dependent part of v_1 , which we denote \bar{v}_1 , satisfies the Rayleigh equation

$$(\bar{u} - c)(\bar{v}_1'' - \bar{\alpha}^2 \bar{v}_1) - \bar{u}'' \bar{v}_1 = 0, \quad (2.8)$$

where $\bar{\alpha} = (\alpha^2 + \beta^2)^{1/2}$.

For the mixing layer profile $\bar{u} = \tanh y$, Curle (1956) has found the following neutral solution of the eigenvalue problem consisting of (2.8) and the boundary conditions that $\bar{v}_1 \rightarrow 0$ as $y \rightarrow \pm\infty$:

$$\bar{v}_1 = \text{sech } y, \quad \bar{\alpha}^2 = \alpha^2 + \beta^2 = 1 \quad \text{and} \quad c = 0. \quad (2.9)$$

We employ this basic solution to construct an initial disturbance of the form

$$\begin{aligned} v^{(1)} = & \{A_{20}(T)e^{i\alpha x} + A_{20}^*e^{-i\alpha x}\}\bar{v}_1(y) \\ & + \{A_{11}(T)e^{i\alpha x/2} + A_{11}^*e^{-i\alpha x/2}\}\bar{v}_1(y) 2 \cos \beta z, \end{aligned} \quad (2.10)$$

where \bar{v}_1 is given by (2.9) and T is a slow time scale. The disturbance can be described as a plane wave plus a subharmonic consisting of two oblique waves of equal amplitude and equally inclined with respect to the mean flow so that in the spanwise direction we have a standing wave. The factor of 2 is introduced because it will simplify the subsequent development to utilize complex exponentials along with the identity $2 \cos \beta z = \exp(i\beta z) + \exp(-i\beta z)$.

A triad of neutral modes satisfying the resonance conditions exactly could be chosen according to (2.9) if $\alpha = 1$ for the plane wave and the subharmonic is comprised of the oblique modes having $\alpha = 1/2$ and $\beta = \pm\sqrt{3}/2$. We depart only slightly from this scheme by allowing the plane wave to be weakly amplified and set

$$\alpha = 1 - \varepsilon^{1/4} \alpha_1. \quad (2.11)$$

From Lin's perturbation formula, the linear growth rate is

$$\alpha c_i = \frac{2}{\pi}(1 - \alpha) = \frac{2}{\pi}\varepsilon^{1/4} \alpha_1$$

and it follows that an appropriate slow time scale is $T = \varepsilon^{1/4} t$.

The procedure for determining the remaining terms in (2.4) - (2.7) will be outlined only briefly because the details are straightforward and in many respects parallel the investigation of Benney (1961). (A principal difference is that Benney employed a steady, viscous critical layer. This, however, has little effect on the first terms of the outer expansion.) When a pair of oblique waves is included in the basic disturbance, then both $u^{(1)}$ and $w^{(1)}$ contain terms having first-order poles at the critical point $y = 0$. For example,

$$w_{11}^{(1)} = -\frac{\sqrt{3}i}{2} A_{11} \operatorname{cosech} y, \quad (2.12)$$

(cf. Section 4 of Benney) where we introduce the notation $w_{lm}^{(n)}$ to mean the term at $O(\varepsilon^{(n-1)/4})$ containing the factor $\exp\{i(\ell x + \sqrt{3}mz)/2\}$.

The presence of singular terms such as that in (2.12) generates discontinuities in certain higher-order velocity components and these must be smoothed out by the critical layer solution. Although the general form of the amplitude equation is determined by the critical layer, the values of coefficients appearing in those equations must be determined by matching to the outer expansion.

Returning now to the expansions (2.4) - (2.7), at $O(\varepsilon^{1/4})$ the quantity $v_{11}^{(2)}$ satisfies a nonhomogeneous Rayleigh equation which can be written

$$\mathcal{L}_1 v_{11}^{(2)} = -2\alpha_1 A_{11} \operatorname{sech} y - 4i A'_{11} \operatorname{sech}^2 y \operatorname{cosech} y, \quad (2.13)$$

where \mathcal{L}_1 is the Rayleigh operator in (2.8) with $\bar{\alpha} = 1$. Because both homogeneous solutions are known in closed form, the method of variation of parameters can be used to write the general solution of (2.13) as

$$v_{11}^{(2)} = C_{11}^{(2)\pm} \text{sech } y + D_{11}^{(2)\pm} (y \text{sech } y + \sinh y) - \alpha_1 A_{11} \cosh y + 2iA'_{11} \left[2\text{sech } y \int_0^y y_1 \text{cosech } 2y_1 dy_1 - (y \text{sech } y + \sinh y) \log(\tanh |y|) \right], \quad (2.14)$$

where \pm denotes above and below the critical layer. Imposing the homogeneous boundary conditions as $y \rightarrow \pm\infty$ shows that there is a jump in $D_{11}^{(2)}$ which is related to the amplitude of the oblique waves by

$$D_{11}^{(2)+} - D_{11}^{(2)-} = 2\alpha_1 A_{11}. \quad (2.15)$$

Equations (2.2) and (2.3) can now be used to solve for $u_{11}^{(2)}$, $w_{11}^{(2)}$ and $p_{11}^{(2)}$.

We next repeat this procedure for the $O(\varepsilon^{1/4})$ terms involving the plane wave. The quantity $v_{20}^{(2)}$ satisfies

$$\mathcal{L}_1 v_{20}^{(2)} = -2\alpha_1 A_{20} \text{sech } y - 2iA'_{20} \text{sech}^2 y \text{cosech } y, \quad (2.16)$$

where \mathcal{L}_1 again is the Rayleigh operator with $\bar{\alpha} = 1$. Using variation of parameters, we obtain the same solution as in (2.14) except that the factor 2 in front of the term in square brackets is absent. Imposing the boundary conditions as $y \rightarrow \pm\infty$ yields the jump condition

$$D_{20}^{(2)+} - D_{20}^{(2)-} = 2\alpha_1 A_{20}. \quad (2.17)$$

It will be seen that matching the jumps in (2.15) and (2.17) to the critical layer solution derived in the following section will lead to the amplitude equations governing the temporal evolution of A_{11} and A_{20} . Before continuing, however, we will note one procedural difference compared with Hickernell (1984) and other papers employing non-equilibrium critical layers. Because an analytical solution was not available for the outer problem, the jump conditions in these papers were derived from a generalization of the usual adjoint orthogonality condition in which it is implicit that an outer solution can be found satisfying the boundary conditions. Here, on the other hand, we employ the procedure described in Section 3 of Benney and Maslowe (1975) and actually find the outer solution. The two procedures should lead to the same result for the amplitude equations.

3. CRITICAL LAYER ANALYSIS.

To obtain evolution equations for A_{20} and A_{11} , we shall now pose an inner expansion in the critical layer in order to obtain expressions for the jumps. To this end, we introduce the inner variables $Y = \varepsilon^{-1/4}y$, $U = \varepsilon^{-1/4}u$, $V = \varepsilon^{-1/2}v$, $W = \varepsilon^{-1/4}w$ and $P = \varepsilon^{-1}p$ inside the critical layer, where it should be recalled that ε was the order of magnitude of the disturbance in the outer expansion, so that the governing equations become

$$U_T + UU_x + VU_Y + WU_z + \varepsilon^{-1/2}P_x = 0 \quad (3.1)$$

$$V_T + UV_x + VV_Y + WV_z + P_Y = 0 \quad (3.2)$$

$$W_T + UW_x + VW_Y + WW_z + \varepsilon^{-1/2}P_z = 0 \quad (3.3)$$

$$U_x + V_Y + W_z = 0. \quad (3.4)$$

The form of the outer solution written in the inner variables suggests that the inner expansion is of the form

$$U = Y + \varepsilon^{1/2}U_2 + \varepsilon^{3/4}U_3 + \varepsilon U_4 + \dots \quad (3.5)$$

$$V = \varepsilon^{1/2}V_2 + \varepsilon^{3/4}V_3 + \varepsilon V_4 + \dots \quad (3.6)$$

$$W = \varepsilon^{1/2}W_2 + \varepsilon^{3/4}W_3 + \varepsilon W_4 + \dots \quad (3.7)$$

$$P = P_0 + \varepsilon^{1/4}P_1 + \varepsilon^{1/2}P_2 + \varepsilon^{3/4}P_3 + \varepsilon P_4 + \dots \quad (3.8)$$

Substituting this expansion into the governing equations, collecting powers of ε and grouping terms with the same x dependence, we arrive at a series of equations of the form

$$\phi_T + i\frac{nY}{2}\phi = \chi(Y, T) \quad (3.9)$$

which have solutions of the form

$$\phi = \int_{-\infty}^T \chi(Y, T_0) e^{\frac{niY}{2}(T_0 - T)} dT_0. \quad (3.10)$$

We will also need to calculate the jumps in several quantities across the critical layer with, for example, the jump in ϕ given by $\int_{-\infty}^{\infty} \phi_Y dY$; when we come to do this, it should be recalled from the definition of the Fourier transform that, for real $a \neq 0$,

$$\int_{-\infty}^{\infty} e^{iaYT} dY = \frac{2\pi}{|a|} \delta(T).$$

For the inner expansion, we shall use the notation $U_{m,n}^{(l)}$ to mean the term at $O(\varepsilon^{l/4})$ accompanying $\exp(i\alpha(mx + n\sqrt{3}z)/2)$; in what follows, we will only give the terms corresponding to non-negative m and n , with the remaining terms following from symmetry: for example, $U_{-2,0}^{(2)} = U_{20}^{(2)*}$. Additionally, only those terms necessary to evaluate the jumps will be determined.

3.1 $O(\varepsilon^{1/2})$ terms.

At this order, we find that, in addition to both the two-dimensional and the oblique waves, there is a non-zero component of the mean flow present in the x -direction, $U_{00}^{(2)} = -Y^3/3$, with $V_{00}^{(2)} = W_{00}^{(2)} = 0$.

For the two-dimensional wave, we find that $U_{20}^{(2)} = W_{20}^{(2)} = 0$ and $V_{20}^{(2)} = A_{20}$, with the relevant pressure terms given by

$$P_{20}^{(0)} = iA_{20} \quad (3.11)$$

$$P_{20}^{(1)} = iC_{20}^{(2)(\pm)} \quad (3.12)$$

$$P_{20}^{(2)} = -\frac{iA_{20}Y^2}{2} - A_{20}'Y + 3iA_{20}'' + i\alpha_1 C_{20}^{(2)(\pm)} + iC_{20}^{(3)(\pm)} - 2D_{20}^{(2)(\pm)'} \quad (3.13)$$

Since $P_{20}^{(1)}$ and $P_{20}^{(2)}$ must be continuous, this tells us that $C_{20}^{(2)(+)} = C_{20}^{(2)(-)} = C_{20}^{(2)}$ and $C_{20}^{(3)(+)} + 2iD_{20}^{(2)(+)' } = C_{20}^{(3)(-)} + 2iD_{20}^{(2)(-)'}$.

For the oblique waves, we find that $V_{11}^{(2)} = A_{11}$ and that $U_{11}^{(2)}$ satisfies

$$U_{11,T}^{(2)} + \frac{iY}{2}U_{11}^{(2)} = -\frac{3}{4}A_{11}$$

with solution $U_{11}^{(2)} = -\frac{3}{4} \int_{-\infty}^T A_{11}(T_0) e^{\frac{iY}{2}(T_0-T)} dT_0$ (3.14)

$$\text{and } W_{11}^{(2)} = -\frac{U_{11}^{(2)}}{\sqrt{3}} = \frac{\sqrt{3}}{4} \int_{-\infty}^T A_{11}(T_0) e^{\frac{iY}{2}(T_0-T)} dT_0 \quad (3.15)$$

with the relevant pressure terms given by

$$P_{11}^{(0)} = \frac{iA_{11}}{2} \quad (3.16)$$

$$P_{11}^{(1)} = \frac{iC_{11}^{(2)(\pm)}}{2} \quad (3.17)$$

$$\text{and } P_{11}^{(2)} = -\frac{iA_{11}Y^2}{4} - A_{11}'Y + 6iA_{11}'' + \frac{i\alpha_1 C_{11}^{(2)(\pm)}}{2} + \frac{iC_{11}^{(3)(\pm)}}{2} - 2D_{11}^{(2)(\pm)'} \quad (3.18)$$

Since $P_{11}^{(1)}$ and $P_{11}^{(2)}$ must be continuous, this tells us that $C_{11}^{(2)(+)} = C_{11}^{(2)(-)} = C_{11}^{(2)}$ and $C_{11}^{(3)(+)} + 4iD_{11}^{(2)(+)' } = C_{11}^{(3)(-)} + 4iD_{11}^{(2)(-)'}$.

3.2 $O(\varepsilon^{3/4})$ terms.

At this order, only the $\exp(i\alpha x)$ terms and the $\exp(i\alpha(x + \sqrt{3}z)/2)$ terms need to be calculated. For the two-dimensional wave, we find that $U_{20}^{(3)} = W_{20}^{(3)} = 0$ and that $V_{20}^{(3)} = C_{20}^{(2)} - \alpha_1 A_{20}(T)$.

For the oblique waves, we find that $V_{11}^{(3)} = C_{11}^{(2)} - \alpha_1 A_{11}/4$ and that

$$\begin{aligned} W_{11,T}^{(3)} + \frac{iY}{2} W_{11}^{(3)} &= -\frac{\sqrt{3}\alpha_1 A_{11}}{4} + \frac{\sqrt{3}C_{11}^{(2)}}{4} - \frac{i\alpha_1 Y U_{11}^{(2)}}{2\sqrt{3}} \\ &= \frac{\sqrt{3}C_{11}^{(2)}}{4} - \frac{\sqrt{3}\alpha_1}{4} \int_{-\infty}^T A'_{11}(T_0) e^{\frac{iY}{2}(T_0-T)} dT_0 \end{aligned} \quad (3.19)$$

which has a solution

$$\begin{aligned} W_{11}^{(3)} &= \frac{\sqrt{3}}{4} \int_{-\infty}^T C_{11}^{(2)}(T_0) e^{\frac{iY}{2}(T_0-T)} dT_0 \\ &\quad + \frac{\sqrt{3}\alpha_1}{4} \int_{-\infty}^T (T_0 - T) A'_{11}(T_0) e^{\frac{iY}{2}(T_0-T)} dT_0, \end{aligned} \quad (3.20)$$

and that

$$\begin{aligned} U_{11,YT}^{(3)} + \frac{iY}{2} U_{11,Y}^{(3)} &= \frac{i\sqrt{3}W_{11}^{(3)}}{2} + \frac{i\alpha_1 Y U_{11,Y}^{(2)}}{2} + \frac{i\alpha_1 U_{11}^{(2)}}{2} \\ &= \frac{3i}{8} \int_{-\infty}^T C_{11}^{(2)}(T_0) e^{\frac{iY}{2}(T_0-T)} dT_0 \\ &\quad - \frac{3\alpha_1 i}{4} \int_{-\infty}^T \int_{-\infty}^{T_1} A'_{11}(T_0) e^{\frac{iY}{2}(T_0-T)} dT_0 dT_1 \end{aligned} \quad (3.21)$$

which has a solution

$$\begin{aligned} U_{11}^{(3)} &= -\frac{3}{4} \int_{-\infty}^T C_{11}^{(2)}(T_0) e^{\frac{iY}{2}(T_0-T)} dT_0 \\ &\quad - \frac{3\alpha_1}{4} \int_{-\infty}^T (T_0 - T) A'_{11}(T_0) e^{\frac{iY}{2}(T_0-T)} dT_0 \end{aligned} \quad (3.22)$$

so that $U_{11}^{(3)} + \sqrt{3}W_{11}^{(3)} = 0$.

3.3 $O(\varepsilon)$ terms.

It is at this order that we shall evaluate the jumps necessary to obtain the evolution equations. For the two-dimensional wave, from the outer, we know that as $Y \rightarrow \pm\infty$,

$$U_{20}^{(4)} + iA_{20}(T)Y \sim 2A'_{20} \log |Y| + A'_{20} + 2iD_{20}^{(2)(\pm)} + O(Y^{-1})$$

so that

$$\begin{aligned} A_{20} &= \frac{1}{2\alpha_1} \left(D_{20}^{(2)(+)} - D_{20}^{(2)(-)} \right) \\ &= \frac{1}{4i\alpha_1} \int_{-\infty}^{\infty} \left(U_{20,Y}^{(4)} + iA_{20} \right). \end{aligned} \quad (3.23)$$

We find that $U_{20}^{(4)}$ satisfies

$$\begin{aligned} \left(\frac{\partial}{\partial T} + iY \right) U_{20,Y}^{(4)} &= -iP_{20,Y}^{(2)} + i\alpha_1 P_{20,Y}^{(1)} - 4iU_{11}^{(2)} U_{11,Y}^{(2)} - 2A_{11} U_{11,Y,Y}^{(2)} \\ &= -\frac{9}{8} \int_{-\infty}^T \int_{-\infty}^T \int_{-\infty}^{T_1} A_{11}(T_0) A_{11}(T_2) e^{\frac{iY}{2}(T_0+T_2-2T)} dT_0 dT_1 dT_2 \\ &\quad - \frac{3}{4} \int_{-\infty}^T \int_{-\infty}^{T_2} \int_{-\infty}^{T_1} A_{11}(T) A_{11}(T_0) e^{\frac{iY}{2}(T_0-T)} dT_0 dT_1 dT_2 \\ &\quad + A_{20}(T)Y + iA'_{20}(T) \end{aligned} \quad (3.24)$$

so that

$$\begin{aligned} &U_{20,Y}^{(4)} + iA_{20} \\ &= \frac{3}{8} \int_{-\infty}^T \int_{-\infty}^{T_1} (-3T^2 + 3TT_0 - T_0^2 + 3TT_1 - T_0T_1 - T_1^2) A_{11}(T_0) A_{11}(T_1) e^{\frac{iY}{2}(T_0+T_1-2T)} dT_0 dT_1 \\ &\quad + 2i \int_{-\infty}^T A'_{20}(T_0) e^{iY(T_0-T)} dT_0 \\ &= -\frac{3}{8} \int_0^\infty \int_0^\infty (\tau_0^2 + 3\tau_0\tau_1 + 3\tau_1^2) A_{11}(T_0) A_{11}(T_1) e^{-\frac{iY}{2}(\tau_0+2\tau_1)} d\tau_0 d\tau_1 \\ &\quad + 2i \int_0^\infty A'_{20}(T - \tau_0) e^{-iY\tau_0} d\tau_0. \end{aligned} \quad (3.25)$$

The jump in $(U_{20}^{(4)}(Y, T) + iA_{20}Y)$ across the critical layer tells us that

$$\begin{aligned} A_{20} &= \frac{1}{4i\alpha_1} \int_{-\infty}^{\infty} \left(U_{20,Y}^{(4)} + iA_{20} \right) dY \\ &= -\frac{3i}{32\alpha_1} \int_{-\infty}^{\infty} \int_0^\infty \int_0^\infty (\tau_0^2 + 3\tau_0\tau_1 + 3\tau_1^2) A_{11}(T - \tau_0 - \tau_1) A_{11}(T - \tau_1) e^{-\frac{iY}{2}(\tau_0+2\tau_1)} d\tau_0 d\tau_1 dY \\ &\quad + \frac{1}{2\alpha_1} \int_{-\infty}^{\infty} \int_0^\infty A'_{20}(T - \tau_0) e^{-iY\tau_0} d\tau_0 dY \\ &= -\frac{3i\pi}{16\alpha_1} \int_0^\infty \int_0^\infty \delta(\tau_0 + 2\tau_1) (\tau_0^2 + 3\tau_0\tau_1 + 3\tau_1^2) A_{11}(T - \tau_0 - \tau_1) A_{11}(T - \tau_1) d\tau_0 d\tau_1 \\ &\quad + \frac{\pi}{\alpha_1} \int_0^\infty \delta(\tau_0) A'_{20}(T - \tau_0) d\tau_0 \\ &= \frac{\pi}{2\alpha_1} A'_{20}(T), \end{aligned}$$

and hence one equation is

$$A_{20} - \frac{\pi}{2\alpha_1} A'_{20} = 0. \quad (3.26)$$

Likewise, for the oblique waves, from the outer, we know that as $Y \rightarrow \pm\infty$,

$$U_{11}^{(4)} + \sqrt{3}W_{11}^{(4)} + 2iA_{11}Y \sim 8A'_{11} \log |Y| + 4A'_{11} + 4iD_{11}^{(2)(\pm)} + O(Y^{-1}),$$

so that

$$\begin{aligned} A_{11} &= \frac{1}{2\alpha_1} \left(D_{11}^{(2)(+)} - D_{11}^{(2)(-)} \right) \\ &= \frac{1}{8i\alpha_1} \int_{-\infty}^{\infty} \left(U_{11,Y}^{(4)} + \sqrt{3}W_{11,Y}^{(4)} + 2iA_{11} \right) dY. \end{aligned} \quad (3.27)$$

We find that

$$\begin{aligned} &\left(\frac{\partial}{\partial T} + \frac{iY}{2} \right) \left(U_{11,Y}^{(4)} + \sqrt{3}W_{11,Y}^{(4)} \right) \\ &= -2iP_{11,Y}^{(2)} + 2i\alpha_1 P_{11,Y}^{(1)} - 2A_{20}(T)U_{11,YY}^{(2)*} - A_{11}(T)U_{00,YY}^{(2)} \\ &= YA_{11}(T) + 2iA'_{11}(T) \\ &\quad - \frac{3}{4} \int_{-\infty}^T \int_{-\infty}^{T_2} \int_{-\infty}^{T_1} A_{20}(T)A_{11}^*(T_0)e^{\frac{iY}{2}(-T_0+T)} dT_0 dT_1 dT_2 \end{aligned}$$

so that

$$\begin{aligned} &U_{11,Y}^{(4)} + \sqrt{3}W_{11,Y}^{(4)} + 2iA_{11} \\ &= 4i \int_{-\infty}^T A'_{11}(T_0)e^{\frac{iY}{2}(T_0-T)} dT_0 \\ &\quad - \frac{3}{8} \int_{-\infty}^T \int_{-\infty}^{T_1} (T_0 - T_1)^2 A_{20}(T_1)A_{11}^*(T_0)e^{\frac{iY}{2}(-T_0+2T_1-T)} dT_0 dT_1 \\ &= 4i \int_0^\infty A'_{11}(T - \tau_0)e^{-\frac{iY\tau_0}{2}} d\tau_0 \\ &\quad - \frac{3}{8} \int_0^\infty \int_0^\infty \tau_0^2 A_{20}(T - \tau_1)A_{11}^*(T - \tau_1 - \tau_0)e^{\frac{iY}{2}(\tau_0-\tau_1)} d\tau_0 d\tau_1. \end{aligned} \quad (3.28)$$

The jump in $\left(U_{11}^{(4)}(Y, T) + \sqrt{3}W_{11}^{(4)}(Y, T) + 2iA_{11}Y \right)$ across the critical layer tells us that

$$\begin{aligned}
A_{11} &= \frac{1}{8i\alpha_1} \int_{-\infty}^{\infty} \left(U_{11,Y}^{(4)} + \sqrt{3}W_{11,Y}^{(4)} + 2iA_{11} \right) dY \\
&= \frac{1}{2\alpha_1} \int_{-\infty}^{\infty} \int_0^{\infty} A'_{11}(T - \tau_0) e^{-\frac{iY\tau_0}{2}} d\tau_0 dY \\
&\quad + \frac{3i}{64\alpha_1} \int_{-\infty}^{\infty} \int_0^{\infty} \int_0^{\infty} \tau_0^2 A_{20}(T - \tau_1) A_{11}^*(T - \tau_1 - \tau_0) e^{\frac{iY}{2}(\tau_0 - \tau_1)} d\tau_0 d\tau_1 dY \\
&= \frac{2\pi}{\alpha_1} \int_0^{\infty} \delta(\tau_0) A'_{11}(T - \tau_0) d\tau_0 \\
&\quad + \frac{3i\pi}{16\alpha_1} \int_0^{\infty} \int_0^{\infty} \tau_0^2 \delta(\tau_1 - \tau_0) A_{20}(T - \tau_1) A_{11}^*(T - \tau_1 - \tau_0) d\tau_0 d\tau_1 \\
&= \frac{\pi}{\alpha_1} A'_{11}(T) + \frac{3i\pi}{16\alpha_1} \int_0^{\infty} \tau_0^2 A_{20}(T - \tau_0) A_{11}^*(T - 2\tau_0) d\tau_0,
\end{aligned} \tag{3.29}$$

and hence the amplitude equation for the oblique waves is

$$A'_{11} - \frac{\alpha_1}{\pi} A_{11} = -\frac{3i}{16} \int_0^{\infty} \tau_0^2 A_{20}(T - \tau_0) A_{11}^*(T - 2\tau_0) d\tau_0. \tag{3.30}$$

4. SOLUTION OF THE AMPLITUDE EQUATIONS.

Equation (3.26) has the obvious solution

$$A_{20}(T) = a_{20} e^{2\alpha_1 T/\pi}, \tag{4.1}$$

where a_{20} is a constant, and substituting this result into (3.30), we obtain

$$A_{11}(T) - \frac{\pi}{\alpha_1} A'_{11}(T) = \frac{3i\pi a_{20}}{16\alpha_1} \int_0^{\infty} \tau_0^2 e^{2\alpha_1(T-\tau_0)/\pi} A_{11}^*(T - 2\tau_0) d\tau_0; \tag{4.2}$$

the left-hand side of this equation suggests that we write $A_{11}(T) = B_{11}(T) e^{\alpha_1 T/\pi}$, which leads to an equation for $B_{11}(T)$ which can be cast in the form

$$B'_{11} = -\frac{3ia_{20}}{128} \int_{-\infty}^T (T - r_0)^2 e^{2\alpha_1 r_0/\pi} B_{11}^*(r_0) dr_0, \tag{4.3}$$

which we can integrate with respect to T to get

$$B_{11}(T) = a_{11} - \frac{ia_{20}}{128} \int_{-\infty}^T (T - r_0)^3 e^{2\alpha_1 r_0/\pi} B_{11}^*(r_0) dr_0, \tag{4.4}$$

where a_{11} is a constant.

4.1 SOLUTION BY ITERATION.

A standard technique for solving equations such as (4.4) is the method of successive approximations (Hildebrand, 1965, §3.9), whereby we solve the equation iteratively, taking $B_{11}^{(0)} = a_{11}$ to be our initial guess, and then for successive iterations taking

$$B_{11}^{(n)}(T) = a_{11} - \frac{ia_{20}}{128} \int_{-\infty}^T (T - r_0)^3 e^{2\alpha_1 r_0/\pi} B_{11}^{(n-1)*}(r_0) dr_0, \quad (4.5)$$

which leads to a solution in the form of a series

$$B_{11}(T) = \sum_{m=0}^{\infty} \beta_m e^{2m\alpha_1 T/\pi}, \quad (4.6)$$

with $\beta_0 = a_{11}$ and $\beta_m = -3ia_{20}\beta_{m-1}^* \pi^4 / (2^{10} m^4 \alpha_1^4)$. The ratio test tells us that this series converges absolutely for all $T < \infty$. We can write this series for B_{11} as

$$\begin{aligned} B_{11}(T) = & \frac{1}{2} \left(a_{11} + ia_{11}^* e^{i \arg(a_{20})} \right) \sum_{m=0}^{\infty} \frac{1}{(m!)^4} \left(-\frac{3 |a_{20}| \pi^4}{2^{10} \alpha_1^4} e^{2\alpha_1 T/\pi} \right)^m \\ & + \frac{1}{2} \left(a_{11} - ia_{11}^* e^{i \arg(a_{20})} \right) \sum_{m=0}^{\infty} \frac{1}{(m!)^4} \left(\frac{3 |a_{20}| \pi^4}{2^{10} \alpha_1^4} e^{2\alpha_1 T/\pi} \right)^m. \end{aligned} \quad (4.7)$$

It follows that in order to evaluate B_{11} , we must evaluate the series $\sum_{m=0}^{\infty} x^m / (m!)^4$. We know (Abramowitz & Stegun, 1964) that

$$J_0^2(z) = \sum_{m=0}^{\infty} \frac{(-1)^m (2m)! (\frac{1}{4} z^2)^m}{(m!)^4}$$

and

$$\frac{1}{(2m)!} = \frac{i}{2\pi} \int_C (-p)^{-2m-1} e^{-p} dp, \quad (4.8)$$

the latter of which is Hankel's contour integral, where C starts at $+\infty$ on the real axis, circles the origin in the counterclockwise direction, and returns to the starting point. It follows that

$$\sum_{m=0}^{\infty} \frac{(\frac{1}{4} x^2)^m}{(m!)^4} = \sum_{m=0}^{\infty} \left(\frac{(\frac{1}{4} x^2)^m (2m)!}{(m!)^4} \right) \times \left(\frac{1}{(2m)!} \right) = -\frac{i}{2\pi} \int_C \frac{e^{-p}}{p} J_0^2 \left(\frac{ix}{p} \right) dp \quad (4.9)$$

so that

$$\begin{aligned} B_{11}(T) = & -\frac{i}{4\pi} \left(a_{11} + ia_{11}^* e^{i \arg(a_{20})} \right) \int_C \frac{e^{-p}}{p} J_0^2 \left(\frac{\sqrt{3} \sqrt{|a_{20}|} \pi^2 e^{\alpha_1 T/\pi}}{2^4 \alpha_1^2 p} \right) dp \\ & - \frac{i}{4\pi} \left(a_{11} - ia_{11}^* e^{i \arg(a_{20})} \right) \int_C \frac{e^{-p}}{p} J_0^2 \left(\frac{\sqrt{3} \sqrt{|a_{20}|} \pi^2 e^{\alpha_1 T/\pi}}{2^4 \alpha_1^2 p} \right) dp. \end{aligned} \quad (4.10)$$

4.2 ASYMPTOTIC SOLUTION FOR LARGE T .

In order to evaluate the large T behavior of (4.10), it is necessary to evaluate

$$\int_C \frac{e^{-p}}{p} J_0^2 \left(\frac{x}{p} \right) dp \quad (4.11)$$

and

$$\int_C \frac{e^{-p}}{p} I_0^2 \left(\frac{x}{p} \right) dp \quad (4.12)$$

as $x \rightarrow \infty$. If we set $p = qx$ in (4.11), it becomes

$$\int_C \frac{e^{-qx}}{q} J_0^2 \left(\frac{1}{q} \right) dq = \int_C e^{-qx - \log q} J_0^2 \left(\frac{1}{q} \right) dq. \quad (4.13)$$

Since $w(x, q) = -qx - \log q$ has a saddle point at $q = -1/x$, we can evaluate the large x behavior of (4.13) by setting

$$q = -\frac{1}{x} - \frac{iq_0}{x}, \quad (4.14)$$

which tells us that

$$\int_C \frac{e^{-p}}{p} J_0^2 \left(\frac{x}{p} \right) dp \sim ie \int_{-\infty}^{\infty} e^{-q_0^2/2} J_0^2(-x) dq_0 \sim ie\sqrt{2\pi} J_0^2(x). \quad (4.15)$$

Following a similar procedure with (4.12) tells us that

$$\int_C \frac{e^{-p}}{p} I_0^2 \left(\frac{x}{p} \right) dp \sim ie\sqrt{2\pi} I_0^2(x). \quad (4.16)$$

Now, as $x \rightarrow \infty$, we know (Abramowitz & Stegun, 1964) that

$$\begin{aligned} J_0^2(x) &\sim \frac{1}{\pi x} (\sin 2x + 1) \\ I_0^2(x) &\sim \frac{e^{2x}}{\pi x}, \end{aligned} \quad (4.17)$$

so that

$$\begin{aligned} \int_C \frac{e^{-p}}{p} J_0^2 \left(\frac{x}{p} \right) dp &\sim \frac{i\sqrt{2}e(\sin 2x + 1)}{\sqrt{\pi x}} \\ \int_C \frac{e^{-p}}{p} I_0^2 \left(\frac{x}{p} \right) dp &\sim \frac{i\sqrt{2}e^{1+2x}}{\sqrt{\pi x}}, \end{aligned} \quad (4.18)$$

and therefore our expression for $B_{11}(T)$, namely (4.10), tells us that as $T \rightarrow \infty$,

$$\begin{aligned} B_{11} &\sim \frac{2^{5/2} \alpha_1^2 e(a_{11} + ia_{11}^* e^{i \arg(a_{20})})}{\pi^{7/2} \sqrt{3} \sqrt{|a_{20}|}} e^{\alpha_1 T/\pi} \left(1 + \sin \left(\frac{\sqrt{3} \sqrt{|a_{20}|} \pi^2 e^{\alpha_1 T/\pi}}{8\alpha_1^2} \right) \right) \\ &+ \frac{2^{5/2} \alpha_1^2 e(a_{11} - ia_{11}^* e^{i \arg(a_{20})})}{\pi^{7/2} \sqrt{3} \sqrt{|a_{20}|}} e^{\alpha_1 T/\pi} \exp \left(\frac{\sqrt{3} \sqrt{|a_{20}|} \pi^2 e^{\alpha_1 T/\pi}}{8\alpha_1^2} \right). \end{aligned} \quad (4.19)$$

Since we set $A_{11}(T) = B_{11}(T)e^{\alpha_1 T/\pi}$, we have an expression for A_{11} as $T \rightarrow \infty$,

$$A_{11}(T) \sim \frac{2^{5/2}\alpha_1^2 e(a_{11} + ia_{11}^* e^{i\arg(a_{20})})}{\pi^{7/2}\sqrt{3}\sqrt{|a_{20}|}} \left(1 + \sin\left(\frac{\sqrt{3}\sqrt{|a_{20}|}\pi^2 e^{\alpha_1 T/\pi}}{8\alpha_1^2}\right)\right) + \frac{2^{5/2}\alpha_1^2 e(a_{11} - ia_{11}^* e^{i\arg(a_{20})})}{\pi^{7/2}\sqrt{3}\sqrt{|a_{20}|}} \exp\left(\frac{\sqrt{3}\sqrt{|a_{20}|}\pi^2 e^{\alpha_1 T/\pi}}{8\alpha_1^2}\right). \quad (4.20)$$

If the coefficient in front of the second term in (4.20) is non-zero, $a_{11} \neq ia_{11}^* e^{i\arg(a_{20})}$, then the second term will dominate the large T behavior, and we have

$$A_{11}(T) \sim \frac{2^{5/2}\alpha_1^2 e(a_{11} - ia_{11}^* e^{i\arg(a_{20})})}{\pi^{7/2}\sqrt{3}\sqrt{|a_{20}|}} \exp\left(\frac{\sqrt{3}\sqrt{|a_{20}|}\pi^2 e^{\alpha_1 T/\pi}}{8\alpha_1^2}\right) \quad (4.21)$$

and we will have so-called e^T growth. However, when $a_{11} = ia_{11}^* e^{i\arg(a_{20})}$, so that the second term in (4.20) vanishes, we are left with

$$A_{11}(T) \sim \frac{2^{7/2}\alpha_1^2 e}{\pi^{7/2}\sqrt{3}\sqrt{|a_{20}|}} \left(1 + \sin\left(\frac{\sqrt{3}\sqrt{|a_{20}|}\pi^2 e^{\alpha_1 T/\pi}}{8\alpha_1^2}\right)\right), \quad (4.22)$$

so that as $T \rightarrow \infty$, the oblique waves stop growing and rather oscillate about a fixed value. This corresponds to the shredding interaction discussed in Section 1.

5. CONCLUDING REMARKS.

In the preceding sections, we have investigated the weakly nonlinear interaction of a triad of modes comprised of a plane fundamental and a pair of oblique subharmonics that in the linear neutral limit satisfy the resonance conditions exactly. This has enabled us to carry out a rational asymptotic analysis of the interaction; when only two-dimensional waves are included this cannot be done. Singularities that occur at the critical point have been resolved using a non-equilibrium critical layer that evolves slowly because the plane wave is weakly amplified on a linear basis. To the order of our analysis, the exponential amplification of the plane wave is not altered by the interaction and, for that reason, we term this a parametric resonance. The common amplitude of the oblique waves, on the other hand, satisfies an integro-differential equation, namely, (3.30). This is in contrast to the more conventional resonant interaction theory which employs a viscous critical layer, an εt slow time scale instead of the present $\varepsilon^{1/4}t$, and leads to a pair of coupled nonlinear ordinary differential equations [see, e.g., eqs. (1) of Collins and Maslowe (1988)].

Both an exact and a long-time asymptotic solution of (3.30) were found in Section 4. Of particular interest is the asymptotic result (4.21) showing very rapid growth of the oblique waves for $T \gg 1$. This raises the question of the extent to which such amplification might be observed in a numerical solution of the full Navier-Stokes equations. Although many numerical simulations of unstable mixing layers have been reported in recent years, none employs initial conditions that would permit the resonance studied here to be observed. However, several computational papers are at least indirectly related to our own work in that both oblique and plane wave perturbations were superimposed on a plane mixing layer. These include articles by Metcalfe *et al.* (1987), Moser and Rogers (1993) and Klaassen and Peltier (1989). In each of these papers, significant three-dimensional instabilities were reported, the third differing from the first two in that a Floquet analysis was employed. Unfortunately, these papers all view the three-dimensional perturbations as secondary instabilities, whereas in our analysis the amplitude of the oblique waves is the same order of magnitude as the plane wave.

Nonetheless, Metcalfe *et al.* have considered a set of initial conditions that is, in some sense, related to our own. In particular, results depicted in Figures 12 and 13 of their paper correspond to the initial superposition of a plane wave with $\alpha = 0.4$, a subharmonic with $\alpha = 0.2$ and a pair of oblique waves having $(\alpha, \beta) = (0.4, \pm 0.2)$. The Reynolds number in these computations was 400 which from a stability standpoint is practically inviscid. Although the wavenumbers seem, at first glance, to correspond to modes that are too highly amplified for comparison with our theory, the thickness of the mixing layer doubles during the computation so that at some point they are not far from the linear neutral values.

On the basis of weak nonlinear interactions, it could be argued that the subharmonic and oblique modes interact to produce a subharmonic resembling our own except that the angle of inclination to the flow direction would be 45° instead of 60° . This discrepancy is not serious and could be accounted for by modifying the coefficient of the linear A_{11} term in (3.30). What really precludes any direct comparison with the present theory is that the amplitude of the plane wave in the simulations of Metcalfe *et al.* is several orders of magnitude larger than the oblique and subharmonic perturbations. Even so, after a period of time the amplitudes of both subharmonic and oblique modes become comparable to the fundamental. This is especially true in Figure 12 which pertains to a case where the oblique modes have a much larger initial amplitude than the subharmonic.

Given that even if it is not the case initially the amplitude of the oblique waves can become larger than that of the plane wave according to our analysis (and the numerical simulations do not dispute this) a different scaling in which the oblique waves have a larger amplitude may be appropriate. Such a distinguished limit has been identified by Goldstein and Lee (1992) in their study of the adverse pressure gradient boundary layer [see, also, Wu (1992) for a subsequent application to the Stokes layer]. This scaling leads to coupled nonlinear integro-differential equations for the amplitudes which develop a singularity that signals the onset of a possibly fully nonlinear stage. The singularity appears, in fact, even in the earlier work of Goldstein and Choi (1989) where only the pair of oblique waves was present without a plane wave.

We have formulated this sort of theory for the mixing layer and are presently preparing a paper on that topic. The amplitudes of the oblique and plane waves are taken to be, respectively, $O(\varepsilon)$ and $O(\varepsilon^{4/3})$ and the slow time scale becomes $\varepsilon^{1/3}t$ instead of the present $\varepsilon^{1/4}t$. These scales are identical to those employed by Wu (1992). When the amplitude of the oblique waves is taken to be small compared with the plane wave the new amplitude equations reduce to those of the parametric resonance stage, as was shown by both Wu (1992) and Goldstein and Lee (1992).

Finally, some comments about the spatial case are appropriate due to its relevance to experiments. As discussed in the Appendix of Kelly (1967), it is necessary that u_m be greater than zero to have spatial growth and so we discuss the case $u_m = 1$. In a frame of reference moving with the real phase speed (if it were the same for both the oblique and plane waves), the evolution equations (3.26) and (3.30) would be unchanged except that the independent variable would be $X = \varepsilon^{1/4}x$ instead of T .

An important difference, however, between the spatial and temporal cases is that spatial modes are dispersive for the mixing layer profile (2.1), whereas unstable temporal modes always have $c_r = u_m$. Numerical computations for the spatial case with $u_m = 1$ [see, e.g., Figure 3 of Maslowe and Kelly (1971)] show that c_r does not differ greatly from 1 except for relatively long waves with $\alpha < 0.4$ and this is why numerical simulations of the temporal case seem to yield results that can be compared with experiments. In some of the experiments reported to date, the spanwise wavenumber β is small (although it can vary with downstream distance), so the angle of the oblique waves' inclination is not close to the 60° in our analysis. However, provided that the dispersion is not large, the present analysis could easily be modified to take into account detuning and this should be done if

comparisons were to be made with a particular experiment.

For the nearly neutral modes considered in this paper, the difference in phase speeds in the case $u_m = 1$ turns out to be negligible and could be completely eliminated by having the inclination of the oblique waves increased slightly. If we write

$$c = 1 - \varepsilon^{1/4} c_1, \quad (5.1)$$

then for the plane wave $c_1 = 4\alpha_1/\pi^2$, whereas for the oblique waves $c_1 = 4.5\alpha_1/\pi^2$.

ACKNOWLEDGMENTS

The authors are pleased to acknowledge discussions with Dr. M.E. Goldstein and Dr. L.S. Hultgren most helpful to this research supported both by an FCAR grant from the Ministère de l'Éducation du Québec and the National Sciences and Engineering Research Council of Canada.

References

- Abramowitz, M. and Stegun, I.A., *Handbook of Mathematical Functions*, Dover Publications, Minneola, N.Y., 1965.
- Benney, D.J., *A non-linear theory for oscillations in a parallel flow*, J. Fluid Mech. **10**(209-236), 1961.
- Benney, D.J. and Maslowe, S.A., *The evolution in space and time of nonlinear waves in parallel shear flows*, Stud. Appl. Math. **54**(1975), 181-205.
- Collins, D.A. and Maslowe, S.A., *Vortex pairing and resonant wave interactions in a stratified free shear layer*, J. Fluid Mech. **191** (1988), 465-480.
- Curle, N. *Hydrodynamic stability of the laminar mixing region between parallel streams*, Aero. Res. Coun. unpublished report 18426 (1956).
- Goldstein, M.E. and Choi, S.-W. *Nonlinear evolution of interacting oblique waves on two-dimensional shear layers*, J. Fluid Mech. **207**(1989), 97-120.
- Goldstein, M.E. and Lee, S.S., *Fully coupled resonant- triad interaction in an adverse-pressure gradient boundary layer*, J. Fluid Mech. **245**(1992), 523-551.
- Hickernell, F.J., *Time-dependent critical layers in shear flows on the beta-plane*, J. Fluid Mech. **142**(1984), 431-449.
- Hildebrand, F.B., *Methods of Applied Mathematics* (2nd ed.), Prentice-Hall, Englewood Cliffs, N.J., 1965.
- Ho, C.-M. and Huerre, P., *Perturbed free shear layers*, Ann. Rev. Fluid Mech. **16**(365-424), 1984.
- Huang, L.-S. and Ho, C.-M., *Small-scale transition in a plane mixing layer*, J. Fluid Mech. **210**(475-500), 1990.
- Hultgren, L.S., *Nonlinear spatial equilibration of an externally excited instability wave in a free shear layer*, J. Fluid Mech. **236**(635-664), 1992.

- Hussein, H.S. and Hussein, F., *Subharmonic resonance in a shear layer*, Advances in Turbulence 2 (eds. H.-H. Fernholz and H.E. Fiedler), pp. 96-101, Springer-Verlag, Berlin, 1989.
- Kelly, R.E., *On the stability of an inviscid shear layer which is periodic in space and time*, J. Fluid Mech. **27**(657-689), 1967.
- Klaassen, G.P. and Peltier, W.R., *The role of transverse secondary instabilities in the evolution of free shear layers*, J. Fluid Mech. **202**(367-402), 1989.
- Maslowe, S.A., *Critical layers in shear flows*, Ann. Rev. Fluid Mech. **18**(405-432), 1986.
- Maslowe, S.A. and Kelly, R.E., *Inviscid instability of an unbounded heterogeneous shear layer*, J. Fluid Mech. **48**(405-415), 1971.
- Metcalf, R.W., Orszag, S.A., Brachet, M.E., Menon, S. and Riley, J.J., *Secondary instability of a temporally growing mixing layer*, J. Fluid Mech. **184**(207-243), 1987.
- Monkewitz, P.A., *Subharmonic resonance, pairing and shredding in the mixing layer*, J. Fluid Mech. **188**(223-252), 1988.
- Moser, R.D. and Rogers, M.M., *The three-dimensional evolution of a plane mixing layer: pairing and transition to turbulence*, J. Fluid Mech. **247**(275-320), 1993.
- Patnaik, P.C., Sherman, F.S. and Corcos, G.M., *A numerical simulation of Kelvin-Helmholtz waves of finite amplitude*, J. Fluid Mech. **73** (215-240), 1976.
- Wu, Xuesong, *The nonlinear evolution of high-frequency resonant-triad waves in an oscillatory Stokes layer at high Reynolds number*, J. Fluid Mech. **245**(553-597), 1992.

REPORT DOCUMENTATION PAGE			Form Approved OMB No. 0704-0188	
Public reporting burden for this collection of information is estimated to average 1 hour per response, including the time for reviewing instructions, searching existing data sources, gathering and maintaining the data needed, and completing and reviewing the collection of information. Send comments regarding this burden estimate or any other aspect of this collection of information, including suggestions for reducing this burden, to Washington Headquarters Services, Directorate for Information Operations and Reports, 1215 Jefferson Davis Highway, Suite 1204, Arlington, VA 22202-4302, and to the Office of Management and Budget, Paperwork Reduction Project (0704-0188), Washington, DC 20503.				
1. AGENCY USE ONLY (Leave blank)		2. REPORT DATE October 1993	3. REPORT TYPE AND DATES COVERED Technical Memorandum	
4. TITLE AND SUBTITLE Parametric Resonant Triad Interactions in a Free Shear Layer			5. FUNDING NUMBERS WU-505-90-5K	
6. AUTHOR(S) R. Mallier and S.A. Maslowe				
7. PERFORMING ORGANIZATION NAME(S) AND ADDRESS(ES) National Aeronautics and Space Administration Lewis Research Center Cleveland, Ohio 44135-3191			8. PERFORMING ORGANIZATION REPORT NUMBER E-8166	
9. SPONSORING/MONITORING AGENCY NAME(S) AND ADDRESS(ES) National Aeronautics and Space Administration Washington, D.C. 20546-0001			10. SPONSORING/MONITORING AGENCY REPORT NUMBER NASA TM-106365 ICOMP-93-35	
11. SUPPLEMENTARY NOTES R. Mallier, McGill University, Department of Mathematics and Statistics, Montreal, Quebec, Canada, H3A 2K6 and S.A. Maslowe, Institute for Computational Mechanics in Propulsion, NASA Lewis Research Center, and McGill University, Department of Mathematics and Statistics, Montreal, Quebec, Canada, H3A 2K6, (work funded under NASA Cooperative Agreement NCC3-233). ICOMP Program Director, Louis A. Povinelli, (216) 433-5818.				
12a. DISTRIBUTION/AVAILABILITY STATEMENT Unclassified - Unlimited Subject Category 34			12b. DISTRIBUTION CODE	
13. ABSTRACT (Maximum 200 words) We investigate the weakly nonlinear evolution of a triad of nearly-neutral modes superimposed on a mixing layer with velocity profile $\bar{u} = u_m + \tanh y$. The perturbation consists of a plane wave and a pair of oblique waves each inclined at approximately 60° to the mean flow direction. Because the evolution occurs on a relatively fast time scale, the critical layer dynamics dominate the process and the amplitude evolution of the oblique waves is governed by an integro-differential equation. The long-time solution of this equation predicts very rapid (exponential of an exponential) amplification and we discuss the pertinence of this result to vortex pairing phenomena in mixing layers.				
14. SUBJECT TERMS Triad interaction; Shear layer; Stability			15. NUMBER OF PAGES 22	
			16. PRICE CODE A03	
17. SECURITY CLASSIFICATION OF REPORT Unclassified	18. SECURITY CLASSIFICATION OF THIS PAGE Unclassified	19. SECURITY CLASSIFICATION OF ABSTRACT Unclassified	20. LIMITATION OF ABSTRACT	